Available online at www.sciencedirect.com

SCIENCE DIRECT®

ELSEVIER

Palaeogeography, Palaeoclimatology, Palaeoecology 228 (2005) 260–277

PALAEO

www.elsevier.com/locate/palaeo

Sediment sources and East Asian monsoon intensity over the last 450 ky. Mineralogical and geochemical investigations on South China Sea sediments

S. Boulay [a,*], C. Colin [a], A. Trentesaux [b], N. Frank [c], Z. Liu [d]

[a] *Laboratoire des Interactions et Dynamique des Environnements de Surface, UMR IDES 8148, Bât. 504, Université Paris-Sud, 91405 Orsay, France*

[b] *Laboratoire de Sédimentologie et Géodynamique, UMR PBDS CNRS, FRE 1818, Université de Lille I, 59655 Villeneuve d'Ascq, France*

[c] *Laboratoire des Sciences du Climat et de l'Environnement, Laboratoire mixte CEA-CNRS, Avenue de la Terrasse, 91198 Gif-sur-Yvette Cedex, France*

[d] *Laboratory of Marine Geology, Tongji University, Shanghai 200092, PR China*

Received 4 June 2004; received in revised form 15 April 2005; accepted 6 June 2005

Abstract

A coupled approach based on clay mineral assemblages and isotopic data (Sr and Nd) of sediment from Ocean Drilling Program (ODP) Site 1145 has been used to trace the sources of sediment feeding the northern part of the South China Sea, and to investigate the evolution of East Asian monsoon intensity over the last 450 ky. Clay mineral assemblages are dominated by illite and smectite, with lesser abundance of chlorite and kaolinite. $^{87}Sr/^{86}Sr$ and $\varepsilon_{Nd}(0)$ isotopic data, combined with the smectite/(illite+chlorite) ratio, indicate that the Pearl River is the main contributor for detrital material to the northern margin of the SCS, with variable continental input of volcanic material derived from the erosion of the Luzon Arc. These inputs follow the low-latitude solar insolation with a 23 ky periodicity, as recorded by a periodic change of the clay mineralogy. For the first time, this study presents a SCS deep-sea sediment high-resolution record of climatic changes in the last 450 ky, showing that smectite/(illite+chlorite) variations are mainly related to changes in the East Asian summer monsoon intensity. Because the mineralogical record is independent of other external forcing phenomena such as global glacial/interglacial oscillations, the smectite/(illite+chlorite) ratio has been used here as a proxy to reconstruct past changes of the South-East Asian summer monsoon intensity.

Keywords: South China Sea; Clay minerals; East Asian monsoon; Pearl River; Luzon Arc; Sediment sources

1. Introduction

The East Asian monsoon is one of the major components of the global climate system. It results

* Corresponding author. Fax: +33 1 69154882.
E-mail address: boulay_sebastien@yahoo.fr (S. Boulay).

0031-0182/$ - see front matter © 2005 Elsevier B.V. All rights reserved.
doi:10.1016/j.palaeo.2005.06.005

in differential land–sea heating between the Western Pacific Warm Pool and the Asian continent, and is characterized by seasonal switch in wind direction, precipitation and runoff (Webster, 1987). During winter months, low temperatures over the Asian continent induce the development of a high-pressure cell over northern Asia. This produces cold and dry winds blowing from Central Asia to the South China Sea and the North Pacific Ocean. Conversely, during the summer, the Asian continent heats up while the ocean stays relatively cool, inducing a low atmospheric pressure cell over central China, a reversal in wind direction and heavy monsoon rainfall over Southeastern Asia (Webster, 1987). At the same time, the seasonal winds direction generates a reversal of the South China Sea surface currents, passing from a cyclonic gyre during the winter monsoon to an anticyclonic gyre during the summer monsoon (e.g., Wang and Wang, 1990).

Until now, most of the palaeoclimatic studies which permit the reconstruction of long-term East Asian paleo-monsoon intensity variations are mainly based on Chinese Loess Plateau deposits using proxies like grain size, magnetic susceptibility or clay mineral distribution (An et al., 1990; Porter and An, 1995; Xiao et al., 1995; Chen et al., 1997; Lu et al., 2000). Similar studies of deep-sea sediments from the Indian Ocean and the South China Sea have seldom been performed. Such reconstructions have shown that during glacial periods the summer monsoon intensity was weaker, whereas the winter monsoon was stronger (Wang and Wang, 1990; Miao et al., 1994; Clemens et al., 1996; Pflaumann and Jian, 1999) with respect to the present conditions. Glacial stages were marked by an increase of aridity over northern Asia and significant eolian dust inputs originating from Chinese deserts were deposited in a wide area including the Central China Loess Plateau and the Pacific Ocean. In contrast, interglacial periods are characterized by a stronger summer monsoon, coupled with strengthened southwestern winds and enhanced monsoon rainfall over the continent (An et al., 1990; Morley and Heuseur, 1997; Lu et al., 1999; Wang et al., 1999).

Over low latitude areas, solar insolation, controlled by the precession of the Earth orbit (23 ky cycle), is considered to be the main factor controlling summer monsoon intensity. It has already widely been studied in marine sediments from the Arabian Sea (e.g., Prell, 1984a,b; Clemens and Prell, 1990; Clemens et al., 1991) and the Bay of Bengal (Colin et al., 1998, 1999). In the South China Sea, before Ocean Drilling Program (ODP) Leg 184, there was no clue linking the East Asian summer monsoon intensity to changes of solar radiation. Monsoonal imprints (23 ky cycles) on the terrigeneous fraction were recorded at ODP Sites 1145 and 1146 (Wehausen and Brumsack, 2002; Kissel et al., 2003).

The South China Sea is a unique area, located between the Pacific Ocean and the Asian Continent. As a semi-enclosed basin in connection with the open ocean, it is able to record both global (glacial/interglacial oscillations) and local (monsoon) climatic changes. This marginal sea is fed by three of the biggest rivers in the world, in terms of sediment load: the Mekong, the Red River and the Pearl River, respectively 160, 130 and 100×10^6 t/y. These sediment inputs have shown that they can provide reliable information about the paleoenvironmental variations affecting the Southeast Asian continent (e.g., Wang et al., 1999; Shipboard Scientific Party, 2000; Wehausen and Brumsack, 2002; Kissel et al., 2003; Liu et al., 2003) and allow reconstruction of the East-Asian monsoon history.

This paper reports for the first time a coupled approach to investigate sedimentation in the South China Sea that combines clay mineralogy and Sr–Nd isotope analyses performed on deep-sea sediments from ODP Site 1145 located on the northern margin of the South China Sea. The aim is to reconstruct the paleoenvironmental changes affecting East Asia during the last 450 ky based on: (1) the discrimination of the sediment source(s) supplying the northern margin of the South China Sea and (2) sediment transport pathways to South China Sea. In the end, a connection between Late Pleistocene climatic changes, i.e., monsoon intensity and/or glacial/interglacial oscillations, and the associated siliciclastic sediment response will be established.

2. Material and methods

The study is based on the terrigeneous fraction of deep-sea core and rivers samples. ODP Site 1145 (19°35.04′N, 117°37.86′E) was drilled at a water

depth of 3175 m on the northern margin of the South China Sea during ODP Leg 184 (Fig. 1, Shipboard Scientific Party, 2000). This site is located about 400 km offshore the Pearl River (also known as Zhujiang) mouth. Between 0 and 75 m composite depth (mcd) the sedimentary record consists of an accumulation of hemipelagic sediment, which is quite homogeneous and dominated by terrigeneous muddy clay with quartz silt and a nannofossil-rich carbonate ooze. Other lithologies are present and contain minor amounts of sponge spicules, diatoms and iron sulfides (Shipboard Scientific Party, 2000). Rivers samples are composed of riverbank sediments from the Pearl, Hanjiang, and Minjiang Rivers (Fig. 1).

Clay mineralogy determinations were performed by standard X-ray diffraction (XRD) on a Philips PW 1729 diffractometer with CuKα radiation and Ni filter, under 40 kV and an intensity of 25 mA. These analyses were obtained on the <2 μm carbonate-free fraction, following the procedure described by Holtzapffel (1985). Defloculation was accomplished by successive washing with distilled water after decarbonation with 0.2 N HCl. Particles smaller than 2 μm were separated by gravitational settling and centrifugation. Three XRD runs were performed on the oriented mounts: (i) untreated; (ii) glycolated (12 h in ethylene glycol); and (iii) heated at 500 °C for two hours. Identification of clay minerals was made according to the position of the (001) series

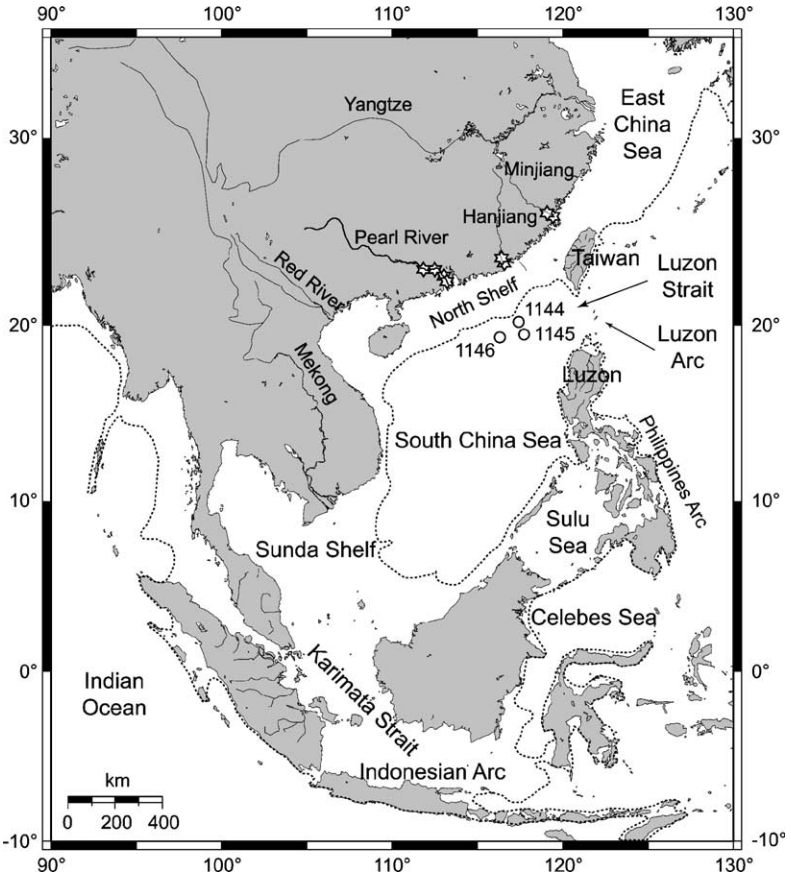

Fig. 1. South China Sea map presenting 1) the location of the ODP Leg 184 drilling sites (white circles); 2) the main tributaries to the South China Sea; and 3) the location of the river's samples analyzed in this study (white stars). Dotted line indicates the isobath −200 m representing the shelf threshold.

of basal reflections on the three XRD diagrams. X-ray diffraction identified illite, chlorite, kaolinite, smectite and complex mixed-layers. These mixed-layer clays were mainly assigned to randomly mixed chlorite–smectite species and will be referred to as "smectite" hereafter. The semi-quantitative composition of the clay fraction was obtained using MacDiff software (Petschick, free-ware available from world wide web) by measuring the peak areas of glycolated samples, for the main clay mineral groups of smectite (smectite+mixed-layers, 15–17 Å), illite (10 Å), and kaolinite/chlorite (7 Å) (Holtzapffel, 1985). Relative proportions of kaolinite and chlorite were determined using the ratio of the 3.57/3.54 Å peak areas.

Although the study of the clay mineralogy is based on the clay size fraction (<2 μm), Sr and Nd isotopic measurements were performed on the total carbonate-free sediment of ODP Site 1145 samples in order to compare our isotopic results to those obtained in previous studies of rocks or carbonate-free sediments from surrounding lands, rivers or marine cores. Such proxies have already been successfully used on marine sediments in order to trace the sources areas of detrital material (e.g., Grousset et al., 1988, 1992; Asahara et al., 1995; Revel et al., 1996; Colin et al., 1999; Fagel et al., 1999; Clift et al., 2002; Li et al., 2003).

The $^{87}Sr/^{86}Sr$ and $^{143}Nd/^{144}Nd$ ratios and concentrations of Sr, Rb and Nd were performed using static multicollection on a Finnigan MAT-262 mass spectrometer at the Laboratoire des Sciences du Climat et de l'Environnement (LSCE, CEA-CNRS, Gif/Yvette). Following the procedure described by Colin et al. (1999), samples were decarbonated by leaching with 20% acetic acid solution in an ultrasonic bath, then rinsed five times and centrifuged to eliminate the carbonate solution. Samples were dissolved in HF–$HClO_4$ and HNO_3–HCl mixtures. The first chemical separation utilized Biorad columns packed with AG50WX-8, 200–400 mesh cation exchange resin. Sr and Rb were then eluted with 2 N HCl and the light rare-earth elements with 2.5 N HNO_3. The Sr fraction was purified on a 20 μl SrSpec® column consisting of a polyethylene syringe with a 4 mm diameter Millex® filter. Nd was isolated by reverse-phase chromatography on HDEHP-coated Teflon powder. $^{87}Sr/^{86}Sr$ ratios were corrected for mass fractionation by normalization to a $^{86}Sr/^{88}Sr$ ratio = 0.1194. Replicate analyses of NIST SRM987 ($n=18$) during the study gave a mean $^{87}Sr/^{86}Sr$ of 0.710240 ± 0.000013 (2σ), close to its certified value of 0.710245. Similarly, $^{143}Nd/^{144}Nd$ ratio was corrected for mass fractionation using a normalization to the natural $^{146}Nd/^{144}Nd$ ratio = 0.7219. Replicate analyses ($n=15$) of a Johnson Matthey internal laboratory standard gave a mean $^{143}Nd/^{144}Nd$ of 0.511097 ± 0.000008, which corresponds to a value of 0.511849 for the La Jolla standard, and is comparable to its certified value of 0.511860. Uncertainties on concentration measurements for Sr, Rb and Nd are <0.1%. Nd isotopic ratios are expressed as $\varepsilon_{Nd}(0) = [((^{143}Nd/^{144}Nd_{meas})/0.512638) - 1] \times 10\,000$, using the CHUR (Chondritic Uniform Reservoir) value given by Jacobsen and Wasserburg (1980).

ODP Site 1145 was sampled at a mean interval of 17 cm along the top 73 mcd and the isotope stratigraphy was established by McIntyre and Oppo (pers.-com.) by correlating the high-resolution $\delta^{18}O$ records of the planktonic foraminifera (*G. ruber*) with the ODP Site 677 (1°12.1380′N, 83°44.2200′W, 3472 m) (Shackleton et al., 1990). The isotope data were run at the Woods Hole Oceanographic Institution using a Finnigan Mat-252 mass spectrometer. ODP Site 1145 was sampled at a 10 cm depth interval in order to analyze clay mineralogy with average temporal resolution of about 1 ky.

3. Results

3.1. Clay mineralogy

For the last 450 ky, illite (24–44%) and smectite (20–58%) are the dominant clay minerals in the ODP Site 1145 sedimentary record (Fig. 2). Chlorite (13–27%) and kaolinite (3–14%) are less abundant. Illite and chlorite contents correlate along a trend that is opposite to the smectite trend (Fig. 2). Variations in kaolinite content are small throughout the record and are within the analytical limits of the method. Though the kaolinite content presents a general trend similar to that of illite and chlorite, its low content and amplitudes allow us to ignore it and thus to use only the smectite/(illite+chlorite) ratio to represent the mineralogical changes within the clay fraction. This

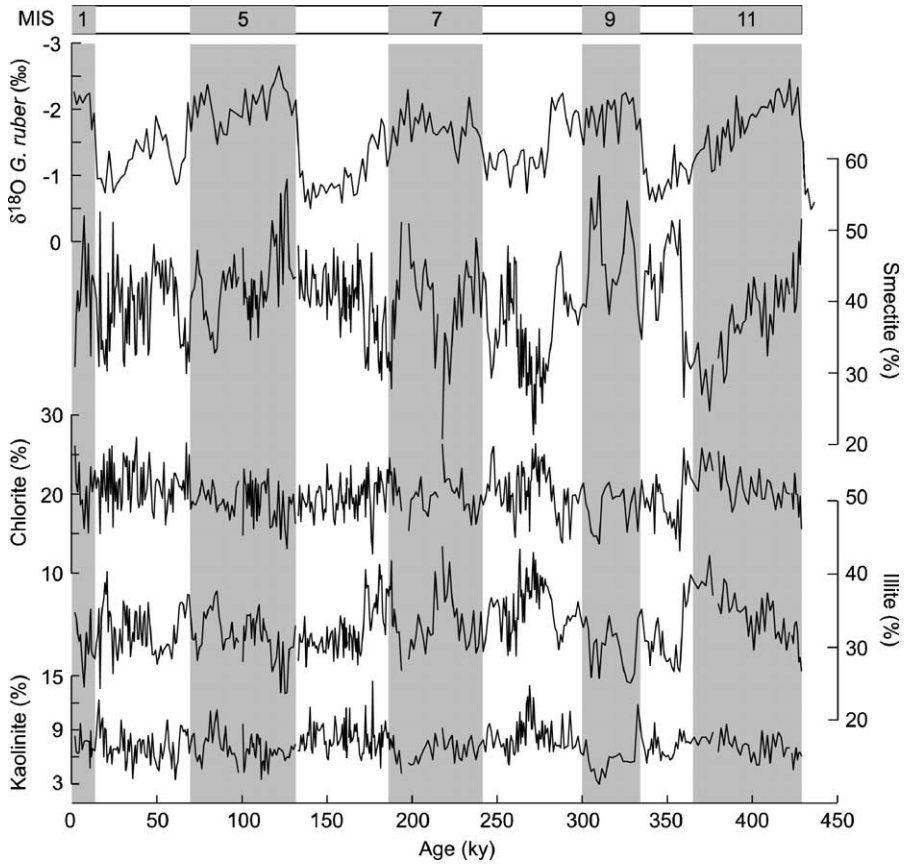

Fig. 2. ODP Site 1145 clay minerals analyses contents (%) obtained on the carbonate-free <2 μm size-fraction for the last 450 ky and compared to the planktonic *G. ruber* δ^{18}O (‰). Illite and smectite are dominant (up to 70% of the total clay minerals). Illite and chlorite follow a similar trend opposed to that of smectite. Kaolinite content do not present any significant variation. Shaded areas mark the marine isotopic stages (MIS).

ratio shows a large variation ranging from 0.30 to 1.55 (Fig. 3).

Nearby ODP Site 1146 (Shipboard Scientific Party, 2000; Fig. 1) has been analyzed at lower resolution (~3 ky), using the same analytical procedure (Trentesaux et al., 2003; Liu et al., 2003). The sediments show the same clay patterns, with similar variations of illite and chlorite contents inversely correlated with smectite. The smectite/(illite+chlorite) has already been found to vary between 0.32 and 1.52 (Liu et al., 2003). A comparison with results of ODP Site 1145 is thus possible (Fig. 3).

A Blackman–Tukey spectral analysis was performed using Analyserie software (Paillard et al., 1996) on the ODP Site 1145 smectite/(illite+chlorite) record. It results in a very high analytical temporal resolution (~1 ky). The power density spectrum reported in Fig. 4 shows significant periodicities at 23, 38, 52, and 114 ky. The periodicity at 23 ky is attributed to the precessional oscillations of the earth's orbit, while those close to 40 and 100 ky are related to the obliquity and eccentricity, respectively. Changes in the mineralogical ratio show a consistent, precession-related oscillation (23 ky), and correlate with the mineralogical variations with calculated September solar radiation at 20°N (Fig. 3). The choice of an insolation curve calculated for September is motivated by the fact that it has already been demonstrated that the summer monsoon intensity variations wasn't correlated with the insolation curve of summer months (June to August) but were linked with September to November insolation curves (depending on the proxy

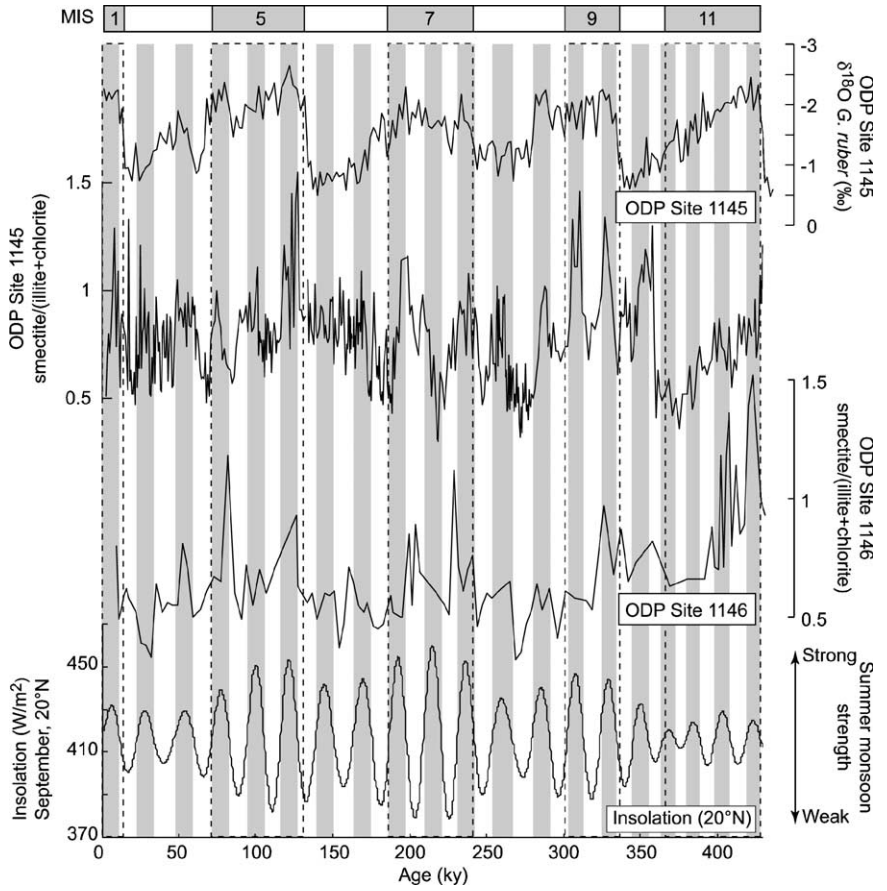

Fig. 3. ODP Site 1145 Planktonic foraminifera (*G. ruber*) $\delta^{18}O$ record (Oppo and McIntyre, pers. com.); smectite/(illite+chlorite) ratios for the ODP Sites 1145 (this study) and 1146 (Liu et al., 2003) over the last 450 ky; and insolation curve calculated for the month of September at the latitude of 20°N (Laskar, 1990). Dotted rectangles mark the MIS while the shaded areas highlight the intervals of maximum insolation. Smectite/(illite+chlorite) ratios do not significantly vary with the glacial/interglacial but are clearly associated to the insolation curve. Each peak of insolation corresponds with an increase of the mineralogical ratio.

used to trace the summer monsoon intensity through times) (e.g., Clemens and Prell, 1990; Beaufort, 1996). This lag between the intensity of the summer month insolation and the summer monsoon intensity is not well explained but such results have been observed in the Andaman Sea (Colin et al., 1999) and gives an calculated September insolation curve in phase with our mineralogical record. Each maximum of the insolation curve corresponds to an increase in the smectite/(illite+chlorite) ratio. On the other hand, the 100 ky-periodicity of the eccentricity, commonly related to Pleistocene glacial/interglacial oscillations, does not seem to be a forcing phenomenon that drives the smectite/(illite+chlorite) 114 ky-periodicity. Consequently, the mineralogical variations do not seem to be associated with the glacial/interglacial shifts (Fig. 3).

The clay mineral analyses performed on riverbank sediments from the Pearl, Hanjiang, and Minjiang Rivers (Fig. 1) show similar assemblages. In every investigated sample, the clay mineralogy is characterized by high proportions of kaolinite (~50%) and illite (~32%). In contrast, chlorite contents are moderate (~15%) and smectite concentration is barely present with 2% of the clay size fraction (Table 1). These Southeast Asian continental results are very distinct from the clay data obtained on ODP Site 1145 sediments in the deep-sea basin (Table 1).

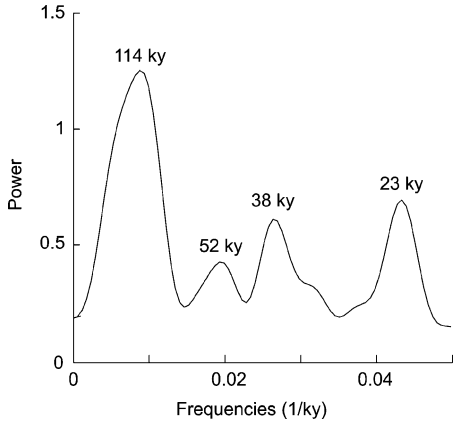

Fig. 4. Blackman–Tukey spectral analysis of ODP Site 1145 smectite/(illite+chlorite) ratio for the last 450 ky. The important intensity of the 23 ky periodicity confirms the relationship between the clay mineralogy and the low latitude solar forcing, and thus the link with the East-Asian summer monsoon intensity.

3.2. Isotopic results

Sr and Nd concentrations, and isotopic ratios measured on the ODP Site 1145 carbonate-free fraction are listed in Table 2. The Sr and Nd concentrations vary between 98–168 and 20–29 ppm, respectively. During the last 450 ky, the $^{87}Sr/^{86}Sr$ ratio and the $\varepsilon_{Nd}(0)$ vary sharply between 0.71137 and 0.72281, and between −8.8 and −11.7, respectively (Fig. 5). These values are consistent with the previously published South China Sea data (Clift et al., 2002; Li et al., 2003) and suggest variations in sedimentary sources. $\varepsilon_{Nd}(0)$ values are inversely related to the $^{87}Sr/^{86}Sr$ ratio: a more radiogenic Sr ratio is associated with less radiogenic $\varepsilon_{Nd}(0)$ values. Moreover, no significant change of $^{87}Sr/^{86}Sr$ ratio or $\varepsilon_{Nd}(0)$ occurs at glacial/interglacial transitions (Fig. 5).

$^{87}Sr/^{86}Sr$ variations are similar to those of the smectite/(illite+chlorite) ratios. An increase of the mineralogical ratio corresponds to a decrease of the $^{87}Sr/^{86}Sr$ ratio (Fig. 5). The clay content variations are related to the summer solar insolation received at low latitudes (20°N), suggesting a tight coupling between the clay mineral distribution and low latitude climatic changes. By comparison with the insolation curve the ODP Site 1145 samples have been separated in two parts corresponding to high and low insolation periods. This allows the $^{87}Sr/^{86}Sr$ ratios, the clay contents, and the monsoon intensity to be compared (Fig. 6). No relationship between $^{87}Sr/^{86}Sr$ and kaolinite content is apparent. On the other hand, trends exist between $^{87}Sr/^{86}Sr$ ratio and illite or smectite contents and to a lesser extent, with chlorite abundance. Samples corresponding to low insolation periods are characterized by higher chlorite and illite contents, and more radiogenic Sr ratio, while those corresponding to strong insolation periods are characterized by high smectite content and low $^{87}Sr/^{86}Sr$ values.

4. Discussion

The sedimentary records at ODP Sites 1145 and 1146 contain similar relative contributions of each clay mineral through time and do not record any change in the nature of these minerals with up to 75

Table 1
Clay mineral proportion (%) on the <2 μm size fraction of sediments from the Pearl, Hanjiang and Minjiang Rivers

Province	Rivers	Sites	Number of samples	Chlorite (%)	Illite (%)	Smectite (%)	Kaolinite (%)
Guangdong	Pearl River	Jiangmen	4	19	34	2	45
Guangdong	Pearl River	Queshang	3	15	32	6	47
Guangdong	Pearl River	Zhaoqing	4	11	25	0	64
Guangdong	Pearl River	Deqing	5	16	36	0	48
Guangdong	Han Jiang	Chenghai	3	5	16	0	79
Guangdong	Han Jiang	Chaozhou	4	5	15	0	80
Fujian	Min Jiang	Mawei	3	8	20	0	71
Fujian	Min Jiang	Minhou	3	11	28	2	59
Mean			29	11	26	1	62
Mean deep-sea assemblage — Site 1145			433	19	32	40	9

Average composition of the Site 1145 clay mineralogy.

Table 2
Rb, Sr and Nd isotopic data measured on the carbonate-free fraction of Site 1145 sediments

Samples	Depth (mcd)	Age (ky)	Sr (ppm)	Rb (ppm)	Nd (ppm)	Rb/Sr	$^{87}Sr/^{86}Sr$	$\pm 2\sigma$ (10^{-5})	$^{143}Nd/^{144}Nd$	$\pm 2\sigma$ (10^{-6})	$\varepsilon_{Nd}(0)$
1145C-1H1 68-70	0.88	7.6	105	159	25	1.52	0.71633	1	0.512099	7	−10.5
1145C-1H1 138-140	1.58	12.5	100	110	22	1.10	0.71698	2	0.512080	8	−10.9
1145C-1H3 18-20	3.38	19.7	98	165	27	1.69	0.71912	1	0.512067	9	−11.1
1145C-1H4 8-10	4.78	24.5	119	125	26	1.05	0.71654	1	0.512082	8	−10.8
1145C-1H5 58-60	6.78	31.3	106	149	–	1.41	0.71742	1	–	–	–
1145B-2H2 18-20	8.58	37.5	104	167	27	1.60	0.71786	1	0.512069	6	−11.1
1145B-2H2 138-140	9.78	41.7	119	135	25	1.14	0.71487	3	0.512105	8	−10.4
1145B-2H4 18-20	11.58	48.5	168	151	–	0.90	0.71462	6	–	–	–
1145B-2H5 8-10	12.98	55.4	103	196	28	1.90	0.72122	1	0.512050	6	−11.5
1145C-2H3 68-70	14.38	61.1	106	154	25	1.45	0.71831	1	0.512083	6	−10.8
1145C-2H4 18-20	15.38	65.1	101	151	29	1.50	0.72227	1	0.512064	8	−11.2
1145C-2H5 68-70	17.38	74.1	105	173	26	1.64	0.71900	1	0.512085	7	−10.8
1145C-2H6 78-80	18.98	84.2	100	186	28	1.87	0.72281	1	0.512060	8	−11.3
1145B-3H2 138-140	19.98	90.6	114	174	27	1.52	0.71885	2	0.512075	8	−11.0
1145B-3H3 68-70	20.78	95.7	109	167	25	1.52	0.71772	1	0.512084	66	−10.8
1145B-3H4 138-140	22.98	109.7	113	175	27	1.54	0.71838	2	0.512079	7	−10.9
1145B-3H5 88-90	23.98	118.1	120	136	21	1.14	0.71480	3	0.512104	9	−10.4
1145B-3H6 8-10	24.68	126.8	109	134	22	1.22	0.71549	1	0.512092	19	−10.7
1145A-4H2 48-50	25.88	138.0	138	136	24	0.99	0.71371	7	0.512090	7	−10.7
1145A-4H3 18-20	27.08	147.3	105	137	25	1.30	0.71712	1	0.512069	9	−11.1
1145A-4H3 108-110	27.98	154.2	109	141	26	1.29	0.71772	1	0.512076	6	−11.0
1145A-4H4 118-120	29.58	161.9	117	136	25	1.17	0.71447	1	0.512186	9	−8.8
1145A-4H5 88-90	30.78	165.4	107	137	26	1.28	0.71802	1	0.512079	8	−10.9
1145C-4H3 8-10	33.93	174.7	106	166	–	1.57	0.72148	1	–	–	–
1145C-4H4 118-120	36.53	182.3	107	174	29	1.63	0.72250	3	0.512048	7	−11.5
1145C-4H5 148-150	38.33	187.6	110	158	27	1.44	0.72026	1	0.512079	7	−10.9
1145B-5H2 118-120	40.33	198.3	108	146	23	1.36	0.71779	1	0.512079	7	−10.9
1145B-5H4 18-20	42.33	212.5	112	173	27	1.55	0.72046	4	0.512052	6	−11.4
1145B-5H5 8-10	43.73	222.4	102	171	28	1.67	0.72109	1	0.512064	7	−11.2
1145B-5H5 148-150	45.13	232.3	126	137	23	1.09	0.71451	1	0.512099	6	−10.5
1145C-5H5 108-110	47.53	248.2	104	166	27	1.59	0.71890	1	0.512039	6	−11.7
1145B-6H2 58-60	49.93	261.5	110	147	24	1.34	0.71755	1	0.512046	5	−11.6
1145B-6H3 88-90	51.73	271.6	103	186	27	1.80	0.72071	1	0.512057	9	−11.3
1145B-6H3 148-150	52.33	275.1	112	165	–	1.48	0.72010	2	–	–	–
1145B-6H5 58-60	54.43	286.5	163	122	20	0.75	0.71137	2	0.512172	9	−9.1
1145C-6H5 58-60	57.83	310.3	123	154	26	1.25	0.71617	1	0.512062	6	−11.2
1145B-7H2 148-150	61.03	340.1	119	–	26	–	0.71649	1	0.512081	8	−10.9
1145B-7H6 108-110	66.43	375.2	112	180	–	1.61	0.71991	1	–	–	–
1145B-8H3 68-70	70.63	409.2	126	141	26	1.12	0.71437	1	0.512128	6	−10.0

$^{87}Sr/^{86}Sr$ ratios have been corrected from mass fractionation using a normalization to a $^{86}Sr/^{88}Sr$ ratio = 0.1194 and $^{143}Nd/^{144}Nd$ to the natural $^{146}Nd/^{144}Nd$ ratio = 0.7219. Nd results are expressed as $\varepsilon_{Nd}(0) = [((^{143}Nd/^{144}Nd_{meas})/0.512638) - 1] \times 1000$, using the present-day CHUR value of Jacobsen and Wasserburg (1980).

m of burial. This indicates that clay minerals have not been altered by early diagenesis and that the clay record does not reflect a localized sedimentation effect on the sea floor, such as migration of deep-sea channel/levee systems. The variation in the composition of clay mineral assemblages thus reflects changing terrigeneous inputs to the South China Sea. Therefore, the sedimentary record can be utilized for paleoenvironmental reconstruction of climatic-driven processes (erosion, weathering, transport) controlling the sedimentary inputs from the surrounding continental areas to the basin. Nevertheless, environmental interpretation of, for example, the smectite/(illite+chlorite) variation must be supported by an understanding of

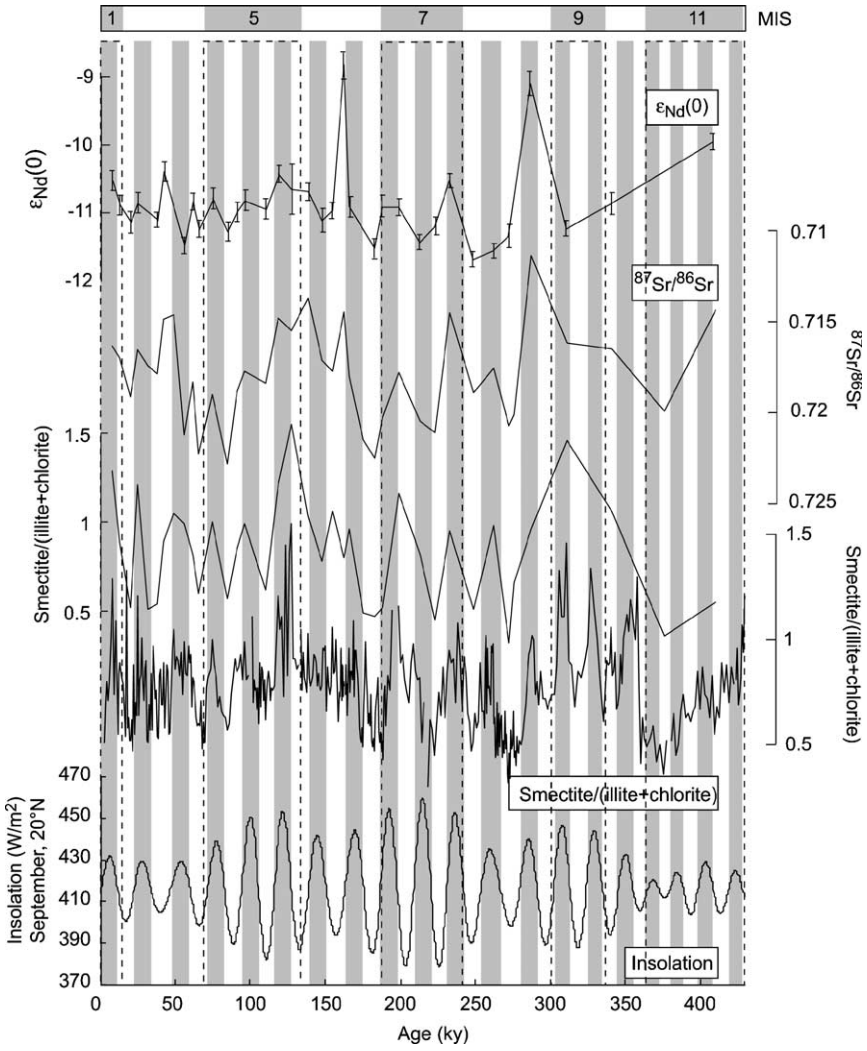

Fig. 5. εNd(0) values, $^{87}Sr/^{86}Sr$ ratio and smectite/(illite+chlorite) ratio measured on the carbonate-free fraction of ODP Site 1145 sediments over the last 450 ky and compared to the insolation curve calculated for September at 20°N (Laskar, 1990). A smectite/(illite+chlorite) ratio curve has been produced with the same time resolution than Sr and Nd isotopic analyses. Dotted rectangles mark the MIS while the shaded areas highlight the intervals of maximum insolation. Large amplitude of variations of εNd(0) values, $^{87}Sr/^{86}Sr$ ratio suggest some changes of sources in the South China Sea northern margin sedimentary records. No particular link can be observed between both data sets and the glacial/interglacial oscillations. High values of $^{87}Sr/^{86}Sr$ are always associated with low εNd(0) values. The $^{87}Sr/^{86}Sr$ variations are similar to those of the smectite/(illite+chlorite) ratio. An increase of the mineralogical ratio corresponds to a decrease of the $^{87}Sr/^{86}Sr$ ratio. This suggests a narrow control of the detrital material sources by the low latitude climatic changes.

the potential source areas as well as the mode and strength of the regional transport mechanisms.

4.1. Pearl River clay minerals inputs

ODP Site 1145 is located ~500 km offshore of the modern Pearl River mouth (Fig. 1). It was probably closer to the paleo-Pearl River estuary (~250 km) during glacial stages as when sea-level was lower by ~110–120 m at the Last Glacial Maximum (LGM) (Wang, 1990; Hanebuth et al., 2000). The Pearl River is one of the major fluviatile sediment source to the South China Sea with an actual mean sediment discharge of $\sim 100 \times 10^6$ t/yr (Zhang et al.,

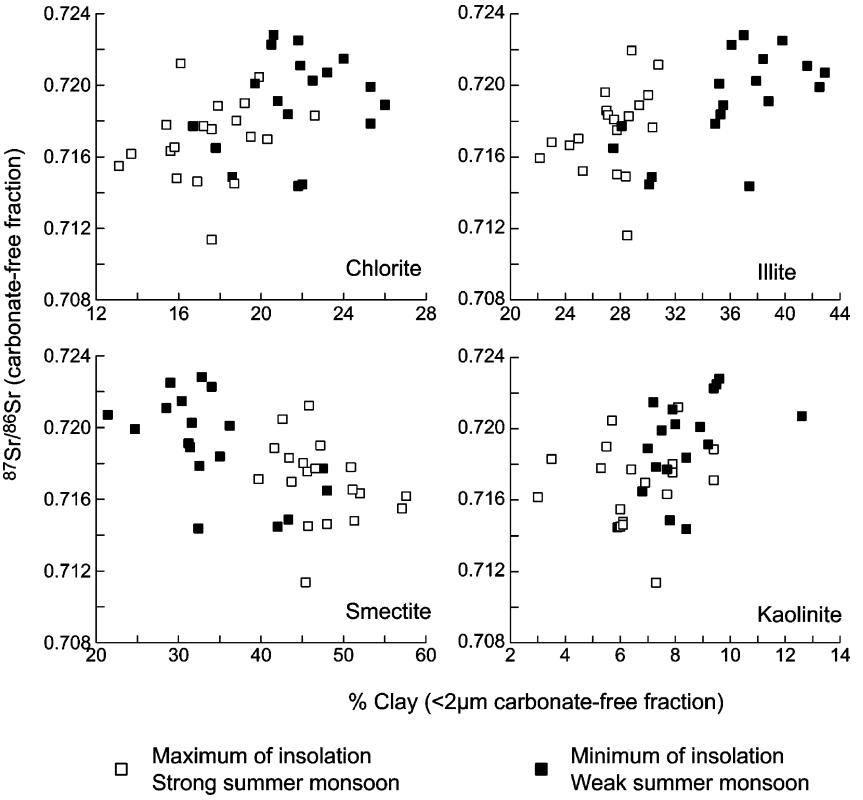

Fig. 6. $^{87}Sr/^{86}Sr$ ratio vs. each clay mineral contents. Open circles correspond to periods of maximum insolation; black dots correspond to periods of weak insolation. Trends exist between $^{87}Sr/^{86}Sr$ ratio and illite–smectite contents. Samples corresponding to low insolation periods are characterized by higher chlorite and illite contents, and more radiogenic Sr ratio than those corresponding to strong insolation periods that are characterized by high smectite content and low $^{87}Sr/^{86}Sr$ values. This result implies a separated origin for smectite and chlorite+illite.

1994, 1999; Lüdmann et al., 2001). The Mekong and the Red River have sediment discharges that are slightly higher than the Pearl River, respectively $\sim 160 \times 10^6$ and $\sim 130 \times 10^6$ t/y. However, given such discharge and considering the distance of these rivers to Sites 1145 and 1146, the Pearl River drainage area is likely the primary source of sediments to the northern South China Sea margin and thus to those sites (Wang et al., 1999; Clift et al., 2002).

The tropical latitude and the relatively low relief of the Pearl River drainage area mean it is subject to limited physical weathering. Soils covering the major part of the Pearl River catchment basin area are dominated by lateritic red earths (ferralitic and bisialitic soils) (Singer, 1988, 1993; Ségalen, 1995; Lan et al., 2003), characteristic of moderate to high chemical weathering, and thus, are a major source of kaolinite and to a lesser extent of smectite. Sediments from the Pearl River, as well as Hanjiang and Minjiang Rivers, contain clay mineral assemblages that are dominated by kaolinite (~50%) and illite (~32%). In contrast, smectite contents are surprisingly low (less than 2%) in all rivers sediments investigated on the Southeast Chinese coast. Thus, the eastern part of the Asian continent could not be the origin of the high smectite clay, reaching more than 55% of the ODP Site 1145 clay fraction (Fig. 2). These mineralogical results are in agreement with the large range of the $^{87}Sr/^{86}Sr$ ratios measured at that site, and with the strong relationship observed between both ratios, smectite/(illite+chlorite) and $^{87}Sr/^{86}Sr$ (Fig. 5). Decreasing smectite and increasing illite–chlorite content in the clay fraction are associated with more radiogenic Sr ratio sediments. Such a correspondence suggests that smectite and illite–chlorite minerals are derived from different sediment sources.

Sediment trap studies in the northern South China Sea have shown that the highest particle fluxes are correlated with high wind speed induced currents rather than river-transported sediments (Jennerjahn et al., 1992; Wiesner et al., 1996). These data confirm that suspended sediments from surrounding landmasses (e.g., the Taiwan or Luzon Islands), eolian particles (e.g., Wang et al., 1999; Wehausen and Brumsack, 2002), or other rivers could have played a significant role in sediment accumulation in the northern part of the South China Sea.

4.2. Potential sources of clay minerals

Two potential sedimentary sources to ODP Site 1145 are the island of Taiwan and the Philippines volcanic arc. Taiwan has one of the highest denudation rates in the world, with a present day value of ~1300 mg/cm^2/yr (Li, 1976) and providing about 400 Mt/yr of sediment to the ocean (only ~150 Mt/yr reaching the South China Sea) (Dadson et al., 2003, 2004). These denudation rates are high enough to prevent minerals to be hydrolyzed prior to erosion, which agrees with the clay mineral contents found in sediments deriving from the erosion of the island. Samples from Taiwan contain high proportion of primary clay minerals (non or slightly hydrolyzed minerals) such as illite (50–60%) and chlorite (30–40%), and negligible concentrations of secondary minerals (moderate to highly hydrolyzed minerals) such as smectite (0–7%) and kaolinite (<3%) (Chamley et al., 1993).

Luzon Island is the northern island of the Philippine archipelago and the only one that is a potential sediment source to the northern part of the South China Sea. The other islands are not directly connected to the South China Sea but are bounded by the Pacific Ocean on one side and the Celebes and Sulu Seas on the other (Fig. 1). Mainly composed of igneous or metamorphic rocks, Luzon produces illite and chlorite (Chen, 1978). Pacific sediments located along the east coast of Luzon are characterized by high contents of chlorite (>25%) (Kolla et al., 1980) but this cannot explain the high smectite contents observed at ODP Site 1145.

Smectite could be derived from the chemical weathering of the volcanic rocks (basalt) (Chamley, 1989) around the South China Sea. A large volume of basalt is present in the volcanic Taiwan–Luzon Arc (including Luzon Island, the Eastern Coastal Range of Taiwan and submarine volcanoes between these two islands) (Fig. 1) and could represent, by weathering, a huge potential source of smectite. Another volcanic formation is the Indonesian Arc that also provides smectitic clay (30–40%) to the Java Sea (Gingele et al., 2001), potentially feeding into the South China Sea through the Borneo Strait. However, the great distance between this arc and ODP Site 1145, and the presence of the wide Sunda Shelf that retains most of the sediment transported northward toward the South China Sea, exclude this from being a significant contributor to the South China Sea smectite.

The East China Sea sediments transported by coastal currents have also been suggested as a sediment source to ODP Site 1146 (Liu et al., 2003). Because of the particular morphology of the South China Sea, the basin was almost completely isolated during low sea-level periods (Wang, 1990; Lüdmann et al., 2001). The water depths in the Taiwan and Karimata Straits (Fig. 1) are quite small and a decrease of 40 m is enough to close the water gateways between the South China Sea and both the East China Sea and the Indian Ocean (Voris, 2000).

ODP Site 1145 clay mineral composition does not exhibit significant glacial/interglacial shifts that would imply episodic sediment inputs from the East China Sea (Fig. 3). Several clues confirm the limited participation of the East China Sea in the South China Sea sedimentary budget: 1) clay minerals assemblages from the East and the South China Sea are very different: East China Sea clay content is characterized by 50–70% illite, 20–40% chlorite, 5–20% kaolinite, and 0–10% of smectite (Aoki et al., 1983; Vagner, 2001); 2) lower sedimentation rates have been calculated during the LGM in the East China Sea (Xu and Oda, 1999) allowing less particles to be transported southward; 3) the continuous presence of the Pacific northward-flowing Kuroshio current, even during glacial stages (studied for the LGM by Xu and Oda (1999)), has probably prevented East China Sea sediments from entering the South China Sea via the Luzon Strait.

Eolian dust, supplied from the Central China Loess Plateau, could also account for the sediment deposition on the northern margin of the South China Sea, as previously reported by Wang et al. (1999), Wehausen and Brumsack (2002), Boulay et al. (2003), and Tamburini et al. (2003). The dominant components in this

eolian material are illite (30–60%) and smectite (10–30%). Kaolinite (1–20%) and chlorite (2–10%) are less abundant (Pesci, 1990). At ODP Site 1145, an average terrigeneous flux of about 10 g/cm^2/ky has been calculated (Boulay, 2004). Assuming a mineral aerosol flux equal to, or less than, the estimated modern value (0.5 g/cm^2/ky) (Duce et al., 1991), the maximum eolian contribution may only account for ~5% of the terrigeneous flux at ODP Site 1145. Thus, the Loess is not a major source of smectite in the South China Sea. We therefore conclude that the main sources of the northern South China Sea sediments are located within the South China Sea and more certainly in its northern part.

4.3. Sediment sources: Isotopic evidence

$^{87}Sr/^{86}Sr$ versus Rb/Sr and $\varepsilon_{Nd}(0)$ versus $^{87}Sr/^{86}Sr$ diagram for the ODP Site 1145 sediments are presented in Fig. 7a and b. Also shown are the published data from potential sedimentary sources: the Pearl River, the Luzon volcanic arc, Taiwan and Chinese loess deposits (Huang et al., 1986; Chen et al., 1990a,b; Defant et al., 1990; Jahn et al., 1990, 2001; Martin et al., 1990; Mukasa et al., 1994; Lan et al., 1995; Pettke et al., 2000). The $^{87}Sr/^{86}Sr$ ratios and $\varepsilon_{Nd}(0)$ values of ODP Site 1145 sediments (Fig. 7) are different from the value of a single Pearl River sample ($^{87}Sr/^{86}Sr=0.7306$; $\varepsilon_{Nd}(0)=-11.8$) (Gaillardet, pers. com.), confirming that the Pearl River is not the only source of sediments to the northern margin of the South China Sea. On the $^{87}Sr/^{86}Sr$ versus Rb/Sr diagram (Fig. 7a), the isotopic data from ODP Site 1145 line up quasi-linearly, linking two potential isotopic end-members. Such results are also confirmed in the $\varepsilon_{Nd}(0)$ versus $^{87}Sr/^{86}Sr$ diagram (Fig. 7b), indicating that each isotopic analysis at ODP Site 1145 is located on a mixing hyperbola linking two end-members. One of them corresponds to the isotopic composition of sediment recovered in the Pearl River. The second end-member of the mixing curves indicates a contribution of sediment with less radiogenic Sr ratios derived from the volcanic arc of Taiwan or Luzon (Fig. 7a and b). Chinese loess isotopic compositions are quite similar to those of Site 1145 sediments (Fig. 7a), but we have seen in agreement with a limited contribution of eolian input to the northern margin of the South China Sea (Boulay, 2004).

Sr and Nd isotopic compositions can distinguish the eastern ($0.70531<{}^{87}Sr/^{86}Sr<0.71358$; $-12.9<\varepsilon_{Nd}(0)<-1$) and the southwestern part ($0.71509<{}^{87}Sr/^{86}Sr<0.72216$; $-15.4<\varepsilon_{Nd}(0)<-9.4$) of Taiwan (Fig. 7b). However, only the rivers of SW Taiwan reach the South China Sea, while the eastern rivers supply the Pacific Ocean and could not be a source for sediment to the Site 1145.

Sr and Nd isotopic composition of sediments from ODP Site 1145 show an alignment and fall in the field from SW Taiwan, except for five samples characterized by lower Sr radiogenic ratios. These could be interpreted as a mixture of sediments from the Pearl River with a strong contribution (more than 90%) of detrital material deriving from the physical erosion of SW Taiwan. Such an interpretation has to be excluded because of the clay minerals results obtained for ODP Sites 1145 and 1146 (Liu et al., 2003) which show high content of smectite (more than 55%) and a strong relationship between smectite contents and $^{87}Sr/^{86}Sr$ ratios. Taiwanese rivers actually discharge sediments mainly composed of illite and chlorite. Nevertheless, because of the closeness of the island and its extreme physical denudation rates, it cannot be totally excluded as a sediment source to the northern margin, but must be considered as a negligible source of smectite to ODP Site 1145.

The isotopic data from ODP Site 1145 are clearly located along a mixing curve linking the Pearl River and the volcanic Luzon Arc end-members (Fig. 7b). Such source areas are in agreement with the polygenetic origin of the clay minerals, with formation of smectite by weathering of volcanic material of the Luzon Arc. This interpretation is well supported by a good correlation between the smectite contents and $^{87}Sr/^{86}Sr$ ratios. Low $^{87}Sr/^{86}Sr$ ratios could reflect an increase of volcanic input (smectite) to the northern margin of the SCS. Taking the average values of the two endmembers, Nd–Sr mass balance consideration suggests that the contribution of the Luzon Arc to the northern margin of the South China Sea could have varied between 3% and 15% of the lithic fraction (Fig. 7b). The large distance between the Luzon Arc and ODP Site 1145 implies that most of the sediment transported to the northern margin of the South China Sea could be in the clay size range and mainly composed of smectite that is able to float for a long time. As the mean proportion of clay fraction is about

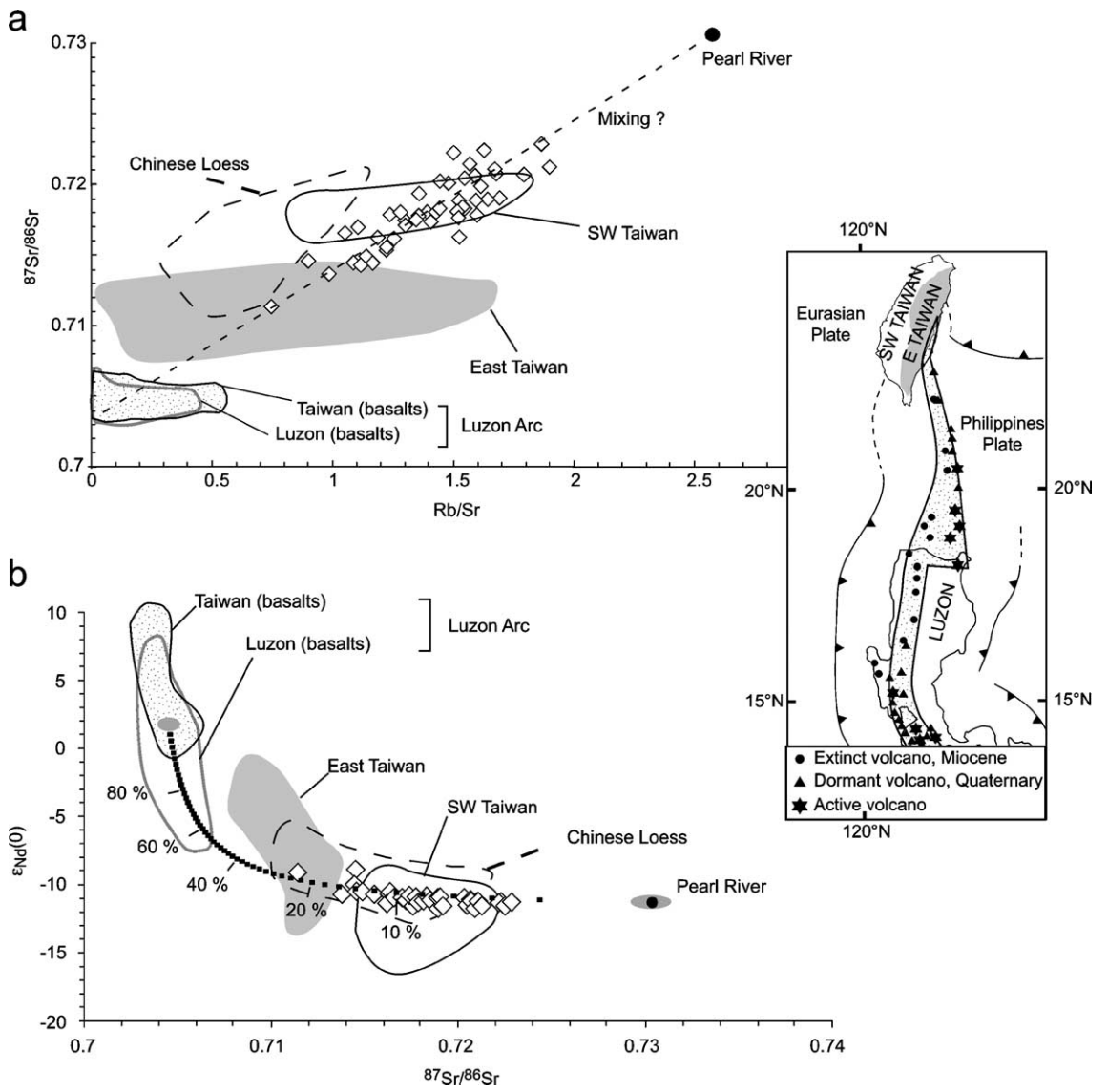

Fig. 7. (a) $^{87}Sr/^{86}Sr$ ratios plotted against Rb/Sr concentration ratios for the detrital component at ODP Site 1145 (white diamonds). Isotopic compositions of the major potential sources to the South China Sea are also reported for comparison. Mixing of sediments on this diagram is presented as a linear array (dotted line); (b) $\varepsilon Nd(0)$ values plotted against $^{87}Sr/^{86}Sr$ ratios for the detrital fraction (white diamonds). Mixing of sediments on this diagram generates an hyperbolic trend between two end-members, the shape of which depends on end-member Sr/Nd ratios. The hyperbolic curve calculated from mean values of Luzon Arc basalts and Pearl River (dotted line) confirms the mixing between these two end-members. Inputs of 3% to 15% of fine sediment from the Luzon arc over the last 450 ky is enough to explain the clay distribution and the isotopic signature of the ODP Site 1145 sediments.

40% of the detrital fraction in ODP Site 1145 (Boulay, 2004), an input of 3–15% of fine sediment from Luzon Arc is enough to explain the clay distribution at this site.

4.4. Climatic significance of clay minerals

The continental shelf in front of the Pearl River mouth is large, up to 300 to 350 km wide. Shelf

transgression and regression occurring during the transition between glacial and interglacial stages might have an important control on sedimentation on northern margin of the South China Sea (Boulay et al., 2003). During low sea-level stands, the continental shelf was exposed. Fluvial sediments were funneled directly to the deep sea. During highstands, sediment was trapped in the delta and adjacent shelf, and coarse clastic deposition was cut off from the South China Sea basin (Boulay, 2004). As Pearl River sediments are mainly composed of illite and kaolinite, such a process would be expressed in glacial sediments of ODP Site 1145 by an increase in the content of these minerals. However, long-term variations in smectite/(illite+chlorite) ratio are not temporally linked to glacial/interglacial shifts, suggesting that sea-level changes do not have a specific impact on the clay transport pattern for the northern part of the South China Sea. This result implies that most of the clay sediments rapidly bypassed the continental shelf without significant alteration during sea-level lowstands.

Smectite/(illite+chlorite) variations also show a strong 23-ky periodicity attributed to the precession of the Earth's orbit (Fig. 4). This periodicity is also well illustrated in Fig. 4 by the correlation between the smectite/(illite+chlorite) ratio and the insolation curve calculated for September at 20°N of latitude. Each maximum of insolation corresponds to an increase in the smectite/(illite+chlorite) ratio. Changes in the smectite/(illite+chlorite) ratio appear to be strongly influenced by the precession cycle. This orbital component is the major forcing mechanism controlling summer monsoon intensity. This periodicity has already been observed in sedimentary records from the western Indian Ocean (Clemens et al., 1991) and the Andaman Sea (Colin et al., 1999), but up to now, no link between the precession and the terrigeneous fraction of deep-sea sediments from the South China Sea has been pointed out. For the first time, the clay mineral analyses from Site 1145 suggest that smectite/(illite+chlorite) variations are mainly related to changes in East Asian summer monsoon intensity.

During the rainy periods associated with the enhanced summer monsoon, precipitation over the entire northern part of the South China Sea stimulates rapid physical erosion and chemical weathering, producing, among others, a large amount of smectite from the volcanic rocks of the Luzon Arc. At the same time, westward advection of these clay particles to ODP Site 1145 requires appropriate oceanic currents. The change in the intensity of the summer and winter monsoon would control the dominant sea-surface pattern of the South China Sea. A summer monsoon increase, relatively to the winter monsoon intensity, could induce a westward current that enter the South China Sea via the Luzon Arc. Up to now, in situ measurements and hydrodynamic models tend to show that surface currents during the summer monsoon exit the South China Sea (e.g., Hu et al., 2000), conflict with the ODP Site 1145 results. It appears also, that intermediate or bottom currents during the summer monsoon flow in the opposite direction to the surface currents, in order to transport smectite to the South China Sea. If such currents exist, their strength would be thus directly correlated with the summer monsoon intensity.

The mineralogical study of ODP Site 1145, through the use of smectite/(illite+chlorite) ratios, demonstrates a strong correspondence between clay content and the precession periodicity. Because no other mechanism, such as the glacial/interglacial oscillations, seems to affect the mineralogical record, the smectite/(illite+chlorite) ratio can be used as an accurate proxy to reconstruct and trace variations of the Southeast Asian paleo-monsoon intensity in the northern part of the South China Sea.

5. Conclusions

High-resolution clay mineralogy, and Sr and Nd isotopic records over the last 450 ky from ODP Site 1145 were analyzed in order to determine sediment sources to the northern margin of the South China Sea and to reconstruct the paleo-strength of the East-Asian monsoon. The results of these analyses suggest the following conclusions.

1) Site 1145 contains four principal clay minerals. Illite and smectite are in the majority, accounting more than 70% of the clay assemblage. Chlorite and kaolinite contents are of secondary importance. Illite and chlorite contents co-vary and are inversely correlated with those of smectite. Kaolinite contents do not vary significantly with time. The

smectite/(illite+chlorite) ratio does not shift with glacial/interglacial oscillations but varies with the September solar insolation curve calculated for 20°N of latitude. Each maximum of the insolation curve corresponds to an increase in the smectite/(illite+chlorite) ratio, suggesting that summer monsoon intensity has a direct control on the clay sedimentation. Both signals are roughly in phase, indicating the rapid response of the system.

2) The mineralogical analyses on the Pearl, Hanjiang and Minjiang Rivers sediments show that kaolinite and illite are dominant, while smectite is absent. This implies that these rivers are not the sources of smectite at ODP Site 1145. The Sr and Nd isotopic compositions of the sediments are also different from those of the Pearl River sediments ($^{87}Sr/^{86}Sr=0.7306$; $\varepsilon_{Nd}(0)=-11.8$). The increase in smectite content are associated with decrease in $^{87}Sr/^{86}Sr$ ratio in the ODP Site 1145 sediments. Sr and Nd isotopic data suggest mixing of two end-members: Pearl River sediments and the volcanic rocks from the Luzon Arc. The main source of the sediment feeding the South China Sea is the Pearl River, but over the last 450 ky, 3% to 15% (mainly composed by smectite) of the total terrigeneous sediment flux was derived from the chemical weathering of Luzon Arc basalts. Sedimentary inputs from the western part of Taiwan are not considered to be a major source of smectite.

3) The smectite/(illite/chlorite) variations are characterized by a strong 23 ky periodicity mainly forced by the low latitude seasonal variation in the solar radiation, linking clay content with the East Asian summer monsoon intensity. During the periods when the summer monsoon is enhanced, physical and chemical weathering of volcanic rocks from the Luzon Arc produced a huge amount of smectite which was probably transported following intermediate or bottom currents. We propose that the smectite/(illite/chlorite) ratio is an accurate proxy for the evolution of the East-Asian summer monsoon in the South China Sea.

Acknowledgments

We thank Kate McIntyre and Delia Oppo for providing the oxygen isotope data. Collection of that data was funded by ODP-USSSP award #F001123. We also thank Ph. Recourt and D. Malengros for their assistance in the performance of clay analyses and M. Allison for helpful review. We specially thank Drs. Bor-ming Jahn, Sylvain Gallet and one anonymous reviewer for their constructive reviews, which significantly helped to improve this work. This study is based on samples provided by the Ocean Drilling Program sponsored by the U.S. National Science Foundation (NSF) and participating countries under management of Joint Oceanographic Institutions (JOI), Inc. Funding for this research was provided by the Centre National de la Recherche Scientifique (CNRS) with the French Program "OCEANS" and by the AFCRST PRA 99-02, which permits us to have helpful discussions with our Chinese colleagues.

References

An, Z., Liu, T., Lu, Y., Porter, S.C., Kukla, G., Wu, X., Hua, Y., 1990. The long-term paleomonsoon variation recorded by the loess–paleosol sequence in central China. Quaternary International 7/8, 91–95.

Aoki, S., Oinuma, K., Okuda, K., Matsuike, K., 1983. Clay mineral composition in surface sediments and the concentration of suspended matter of the East China Sea (in Chinese). Proc. Internat. Symp. on the Continental Shelf. China Ocean Press, pp. 473–482.

Asahara, Y., Tanaka, T., Kamioka, H., Nishimura, A., 1995. Asian continental nature of $^{87}Sr/^{86}Sr$ ratios in north central Pacific sediments. Earth and Planetary Science Letters 133, 105–116.

Beaufort, L., 1996. Dynamics of the monsoon in the equatorial Indian ocean over the last 260,000 years. Quaternary International 31, 13–18.

Boulay, S., 2004. Enregistrements sédimentaires des variations de la mousson sud-est asiatique au cours des 2 derniers millions d'années. University of Paris-XI, Orsay, France. PhD Thesis, 209 pp.

Boulay, S., Colin, C., Trentesaux, A., Pluquet, F., Bertaux, J., Blamart, D., Buehring, C., Wang, P., 2003. Mineralogy and sedimentology of Pleistocene sediment in the South China Sea (ODP Site 1144). In: Prell, W.L., Wang, P., Blum, P., Rea, D.K., Clemens, S.C. (Eds.), Proc. ODP, Sci. Results, vol. 184, pp. 1–21. [Online]. Available from World Wide Web: http://www-odp.tamu.edu/publications/184_SR/VOLUME/CHAPTERS/211.PDF.

Chamley, H., 1989. Clay Sedimentology. Springer-Verlag, Berlin. 623 pp.

Chamley, H., Angelier, J., Teng, L.S., 1993. Tectonic and environmental control of the clay mineral sedimentation in the Late Cenozoic orogen of Taiwan. Geodinamica Acta 6 (2), 135–147.

Chen, P.Y., 1978. Minerals in bottom sediments of the South China Sea. Geological Society of America Bulletin 89, 211–222.

Chen, C.-H., Jahn, B.-M., Lee, T., Chen, C.-H., Cornichet, J., 1990a. Sm–Nd isotopic geochemistry of sediments from Taiwan and implications for the tectonic evolution of southeast China. Chemical Geology 88, 317–332.

Chen, C.-H., Shieh, Y.-N., Lee, T., Chen, C.-H., Mertzman, S.A., 1990b. Nd–Sr–O isotopic evidence for source contamination and unusual mantle component under Luzon Arc. Geochimica et Cosmochimica Acta 54, 2473–2483.

Chen, F.H., Bloemendal, J., Wang, J.M., Li, J.J., Oldfield, F., 1997. High-resolution multi-proxy climate records from Chinese loess: evidence for rapid climatic changes over the last 75 ky. Palaeogeography, Palaeoclimatology, Palaeoecology 130, 323–335.

Clemens, S.C., Prell, W.L., 1990. Late Pleistocene variability of Arabian Sea summer monsoon winds and continental aridity: eolian records from the lithogenic component of deep-sea sediment. Paleoceanography 5 (2), 109–145.

Clemens, S.C., Prell, W.L., Murray, D., Shimmield, G., Weedon, G., 1991. Forcing mechanisms of the Indian Ocean monsoon. Nature 353, 720–725.

Clemens, S.T., Murray, D.W., Prell, W.L., 1996. Nonstationary phase of the Plio-Pleistocene Asian monsoon. Science 274, 943–948.

Clift, P., Lee, J.I., Clark, M.K., Blusztajn, J., 2002. Erosional response of South China to arc rifting and monsoonal strengthening; a record from the South China Sea. Marine Geology 184, 207–226.

Colin, C., Kissel, C., Blamart, D., Turpin, L., 1998. Magnetic properties of sediments in the Bay of Bengal and the Andaman Sea: impact of rapid North Atlantic Ocean climatic events on the strength of the Indian monsoon. Earth and Planetary Science Letters 160, 623–635.

Colin, C., Turpin, L., Bertaux, J., Desprairies, A., Kissel, C., 1999. Erosional history of the Himalayan and Burman ranges during the last two glacial–interglacial cycles. Earth and Planetary Science Letters 171, 647–660.

Dadson, S.J., Hovius, N., Chen, H., Dade, W.B., Hsieh, M.-L., Willet, S.D., Hu, J.-C., M-J., H., Chen, M.-C., Stark, C.P., Lague, D., Lin, J.-C., 2003. Links between erosion, runoff variability and seismicity in the Taiwan orogen. Nature 426, 648–651.

Dadson, S.J., Hovius, N., Chen, H., Dade, W.B., Lin, J.-C., Hsu, M.-L., Lin, C.-W., Horng, M.-J., Chen, T.-C., Milliman, J.D., Stark, C.P., 2004. Earthquake-triggered increase in sediment delivery from an active mountain belt. Geology 32 (8), 733–736.

Defant, M.J., Maury, R.C., Joron, J.L., Feigenson, M.D., Leterrier, J., Bellon, H., Jacques, D., Richard, M., 1990. The geochemistry and tectonic setting of the northern section of the Luzon arc (the Philippines and Taiwan). Tectonophysics 183, 187–205.

Duce, R., Liss, P., Merrill, J., Atlas, E., Buat-Ménard, P., Hicks, B., Miller, J., Prospero, J., Arimoto, R., Church, T., Ellis, W., Galloway, J., Hansen, L., Jickells, T., Knap, A., Reinhardt, K., Schneider, B., Soudine, A., Tokos, J., Tsunogai, S., Wollast, R., Zhou, M., 1991. The atmospherical input of trace species to the world ocean. Global Biogeochemical Cycles 5, 193–259.

Fagel, N., Innocent, C., Stevenson, R.K., Hillaire-Marcel, C., 1999. Deep circulation changes in the Labrador Sea since the Last Glacial Maximum: new constraints from Sm–Nd data on sediments. Paleoceanography 14 (6), 777–788.

Gingele, F.X., De Deckker, P., Hillenbrand, C.-D., 2001. Clay mineral distribution in surface sediments between Indonesia and NW Australia—source and transport by ocean currents. Marine Geology 179, 135–146.

Grousset, F.E., Biscaye, P.E., Zindler, A., Prospero, J., Chester, R., 1988. Neodymium isotopes as tracers in marine sediments and aerosols: north Atlantic. Earth and Planetary Science Letters 87, 367–378.

Grousset, F.E., Rognon, P., Coudé-Gaussen, G., Pédemay, P., 1992. Origins of peri-Saharan dust deposits traced by their Nd and Sr isotopic composition. Palaeogeography, Palaeoclimatology, Palaeoecology 93, 203–212.

Hanebuth, T., Statteger, K., Grootes, P.M., 2000. Rapid flooding of the Sunda Shelf: a Late-Glacial sea-level record. Science 288, 1033–1035.

Holtzapffel, T., 1985. Les minéraux argileux. Préparation, analyse diffractométrique et détermination. University of Lille I, Lille, France. Société Géologique du Nord, Publication n°12, 136 pp.

Hu, J., Kawamura, H., Hong, H., Qi, Y., 2000. A review on the currents in the South China Sea: seasonal circulation, South China Sea warm current and Kuroshio intrusion. Journal of Oceanography 56 (6), 607–624.

Huang, X., Sun, S., DePaolo, D.J., Wu, K., 1986. Nd–Sr isotopic study of Cretaceous magmatic rocks from Fujian province. Acta Petrologica Sinica 2 (2), 50–63 (in Chinese).

Jacobsen, S.B., Wasserburg, G.J., 1980. Sm–Nd isotopic evolution of chondrites. Earth and Planetary Science Letters 50, 139–155.

Jahn, B.-M., Zhou, X.H., Li, J.L., 1990. Formation And Tectonic Evolution Of Southeastern China And Taiwan: Isotopic And Geochemical Constraints. Tectonophysics 183, 145–160.

Jahn, B.-M., Gallet, S., Han, J., 2001. Geochemistry of the Xining, Xifeng and Jixian sections, loess plateau of eolian dust provenance and paleosol evolution during the last 140 ka. Chemical Geology 178, 71–94.

Jennerjahn, T.C., Liebezeit, G., Kempe, S., Xu, L.Q., Chen, W.B., Wang, H.K., 1992. Particle flux in the northern South China Sea. In: Jin, X., Kudrass, H.R., Pautot, G. (Eds.), Marine Geology and Geophysics of the South China Sea. China Ocean Press, Beijing, pp. 228–235.

Kissel, C., Laj, C., Clemens, S., Solheid, P.A., 2003. Magnetic signature of environmental changes in the last 1.2 My at ODP Site 1146, South China Sea. Marine Geology 201, 119–132.

Kolla, V., Nadler, L., Bonatti, E., 1980. Clay mineral distributions in surface sediments of the Philippine Sea. Oceanologica Acta 3 (2), 245–250.

Lan, C.-Y., Lee, T., Jahn, B.-M., Yui, T.-F., 1995. Taiwan as a witness of repeated mantle inputs — Sr–Nd–O isotopic geochemistry of Taiwan granitoids and metapelites. Chemical Geology 124, 287–303.

Lan, H.X., Hu, R.L., Yue, Z.Q., Lee, C.F., Wang, S.J., 2003. Engineering and geological characteristics of granite weathering

profiles in South China. Journal of Asian Earth Sciences 21, 353–364.
Laskar, J., 1990. The chaotic motion of the solar system: a numerical estimate of the size of the chaotic zones. Icarus 88, 266–291.
Li, Y.-H., 1976. Denudation of Taiwan Island since the Pliocene Epoch. Geology 4 (2), 105–107.
Li, X.H., Wei, G., Shao, L., Liu, Y., Liang, X., Jian, Z., Sun, M., Wang, P., 2003. Geochemical and Nd isotopic variations in sediments of the South China Sea: a response to Cenozoic tectonism in SE Asia. Earth and Planetary Science Letters 211, 207–220.
Liu, Z., Trentesaux, A., Clemens, S., Colin, C., Wang, P., Huang, B., Boulay, S., 2003. Clay mineral assemblages in the northern South China Sea: implications for East Asian monsoon evolution over the past 2 million years. Marine Geology 201, 133–146.
Lu, H., Liu, X., Zhang, F., An, Z., Dodson, J., 1999. Astronomical calibration of loess–paleosol deposits at Luochuan, central Chinese Loess Plateau. Palaeogeography, Palaeoclimatology, Palaeoecology 154, 237–246.
Lu, H., van Huissteden, K., Zhou, J., Vandenberghe, J., Liu, X., An, Z., 2000. Variability of East Asian winter monsoon in quaternary climatic extremes in North China. Quaternary Research 54, 321–327.
Lüdmann, T., Wong, H.K., Wang, P., 2001. Plio-Quaternary sedimentation processes and neotectonics of the northern continental margin of the South China Sea. Marine Geology 172, 331–358.
Martin, H., Bonin, B., Capdevila, R., Didier, J., Jahn, J., Lameyre, J., Qiu, Y., Wang, Y., 1990. The Fuzhou granite complex (SE China): petrology and geochemistry. Geochimica 6, 101–111.
Miao, Q., Thunell, R.C., Anderson, D.M., 1994. Glacial–Holocene carbonate dissolution and sea surface temperatures in the South China and Sulu Seas. Paleoceanography 9 (2), 269–290.
Morley, J.J., Heuseur, L.E., 1997. Role of orbital forcing in east Asian monsoon climates during the last 350 ky: evidence from terrestrial and marine climate proxies from core RC14-99. Palaeogeography 12 (3), 483–493.
Mukasa, S.B., Flower, M.F.J., Miklius, A., 1994. The Nd-, Sr- and Pb-isotopic character of lavas from Taal, Laguna de Bay and Arayat volcanoes, southwestern Luzon, Philippines: implications for arc magma petrogenesis. Tectonophysics 235, 205–221.
Paillard, D., Labeyrie, L., Yiou, P., 1996. Analyseries 1.0: a Macintosh software for the analysis of geographical time-series. Eos 77, 123–152.
Pesci, M., 1990. Loess is not just the accumulation of dust. Quaternary International 7–8, 1–21.
Pettke, T., Halliday, A.N., Hall, C.M., Rea, D.K., 2000. Dust production and deposition in Asia and the north Pacific Ocean over the past 12 My. Earth and Planetary Science Letters 178, 397–413.
Pflaumann, U., Jian, Z., 1999. Modern distribution patterns of planktonic foraminifera in the South China Sea and western Pacific: a new transfer technique to estimate regional sea-surface temperature. Marine Geology 156, 41–83.
Porter, S.C., An, Z., 1995. Correlation between climate events in the North Atlantic and China during the last glaciation. Nature 375, 305–308.
Prell, W.L., 1984a. Monsoonal climate of the Arabian Sea during the Late Quaternary: a response to changing solar radiation. In: Berger, A.L. (Ed.), Milankovitch and Climate, vol. 1. D. Riedel, Hingham, MA, pp. 349–366.
Prell, W.L., 1984b. Variation of monsoonal upwelling: a response to changing solar radiation. In: Hansen, J., Takahashi, T. (Eds.), Climate Processes and Climate Sensitivity, vol. 29. American Geophysical Union, pp. 48–57.
Revel, M., Sinko, J.A., Grousset, F.E., Biscaye, P.E., 1996. Sr and Nd isotopes as tracers of North Atlantic lithic particles: paleoclimatic implications. Paleoceanography 11, 95–113.
Ségalen, P. (1995) Les sols ferrallitiques et leur répartition géographique, Tome 1, 2 et 3, ORSTOM Edition.
Shackleton, N.J., Berger, A., Peltier, W.R., 1990. An alternative astronomical calibration of the lower Pleistocene timescale based on ODP Site 677. Transactions of the Royal Society of Edinburgh. Earth Sciences 81, 251–261.
Shipboard Scientific Party, 2000. Leg 184 summary: exploring the Asian monsoon through drilling in the South China Sea. In: Wang, P., Prell, W.L., Blum, J.D. (Eds.), Proc. ODP, Init. Repts., vol. 184. Ocean Drilling Program, College Station TX, pp. 1–77.
Singer, A., 1988. Properties and genesis of some soils of Guanxi Province, China. Geoderma 43, 117–130.
Singer, A., 1993. Weathering patterns in representative soils of Guangxi Province, south-east China, as indicated by detailed clay mineralogy. Journal of Soil Science 44, 173–188.
Tamburini, F., Adatte, T., Föllmi, K., Bernasconi, S.M., Steinmann, P., 2003. Investigating the history of East Asian monsoon and climate during the last glacial interglacial period (0–140,000 years): mineralogy and geochemistry of ODP Site 1143 and 1144, South China Sea. Marine Geology 201, 147–168.
Trentesaux, A., Liu, Z., Colin, C., Boulay, S., Wang, P., 2003. Data report: pleistocene paleoclimatic cyclicity of southern China: clay mineral evidence recorded in the South China Sea (ODP Site 1146). In: Prell, W.L., Wang, P., Blum, P., Rea, D.K., Clemens, S.C. (Eds.), Proc. ODP, Sci. Results, vol. 184, pp. 1–10. [Online]. Available from World Wide Web: http://www-odp.tamu.edu/publications/184_SR/VOLUME/CHAPTERS/210.PDF.
Vagner, P., 2001. Séquences de dépôts du Quaternaire supérieur et variations climatiques en mer Chine de l'est. University of Lille I, Lille, France. PhD Thesis, 247 pp.
Voris, H.K., 2000. Maps of Pleistocene sea levels in Southeast Asia: shorelines, river systems and time durations. Journal of Biogeography 27, 1153–1167.
Wang, P., 1990. The ice-age China Sea. Research results and problems. First International Conference on Asian Marine Geology. China Ocean Press, Shanghai, pp. 181–197.
Wang, L., Wang, P., 1990. Late Quaternary paleoceanography of the South China Sea: glacial–interglacial contrasts in an enclosed basin. Paleoceanography 5 (1), 77–90.
Wang, L., Sarnthein, M., Erlenkeuser, H., Grimalt, J., Grootes, P., Heilig, S., Ivanova, E., Kienast, M., Pelejero, C., Pflaumann, U., 1999. East Asian monsoon climate during the Late Pleistocene: high-resolution sediment records from the South China Sea. Marine Geology 156, 245–284.

Webster, P.J., 1987. The Elementary Monsoon. John Wiley and Sons, New York, pp. 3–32.

Wehausen, R., Brumsack, H.-J., 2002. Astronomical forcing of the East Asian monsoon mirrored by the composition of Pliocene South China Sea sediments. Earth and Planetary Science Letters 201, 621–636.

Wiesner, M.G., Zheng, L., Wong, H.K., Wang, Y., Chen, W., 1996. Flux of particulate matter in the South China Sea. In: Ittikot, V., Schäfer, P., Honjo, S., Depetris, P.J. (Eds.), Particle Flux in the Ocean. John Wiley and Sons, New York, pp. 293–312.

Xiao, J., Porter, S.C., An, Z., Kumai, H., Yoshikawa, S., 1995. Grain size of quartz as an indicator of winter monsoon strength on the Loess Plateau of Central China during the last 130,000 yr. Quaternary Research 43, 22–29.

Xu, X., Oda, M., 1999. Surface-water evolution of the eastern East China Sea during the last 36000 years. Marine Geology 156, 285–304.

Zhang, J., Huang, W., Liu, M., 1994. Geochemistry of major Chinese river–estuary systems. In: Zhou, D., et al., (Eds.), Oceanology of China Seas, vol. 1. Kluwer Academic, Dordrecht, pp. 179–188.

Zhang, J., Yu, Z.G., Wang, J.T., Ren, J.L., Chen, H.T., Xiong, H., Dong, L.X., Xu, W.Y., 1999. The subtropical Zhujiang (Pearl River) estuary: nutrient, trace species and their relationship to photosynthesis. Estuarine, Coastal and Shelf Science 49, 385–400.